Epithermal Gold-Silver Mineralization of the Kitami Metallogenic Province, Hokkaido, Japan

Euis T. YUNINGSIH[1,2] and Hiroharu MATSUEDA[2]

[1.] Faculty of Geology, Padjadjaran University, Bandung, West Java, Indonesia
[2] The Hokkaido University Museum, Hokkaido University, Japan

1. Introduction

The gold-silver mineralization at the Kitami metallogenic province, located at the northeastern Hokkaido, Japan (Figure 1) is occurred in the Neogene Tertiary age. The gold-silver deposits in this district were one of the valuable mining districts in Japan. Epithermal ore deposits of the gold-silver mines in this district present similarities in mineral compositions, vein features, and also their host rocks.

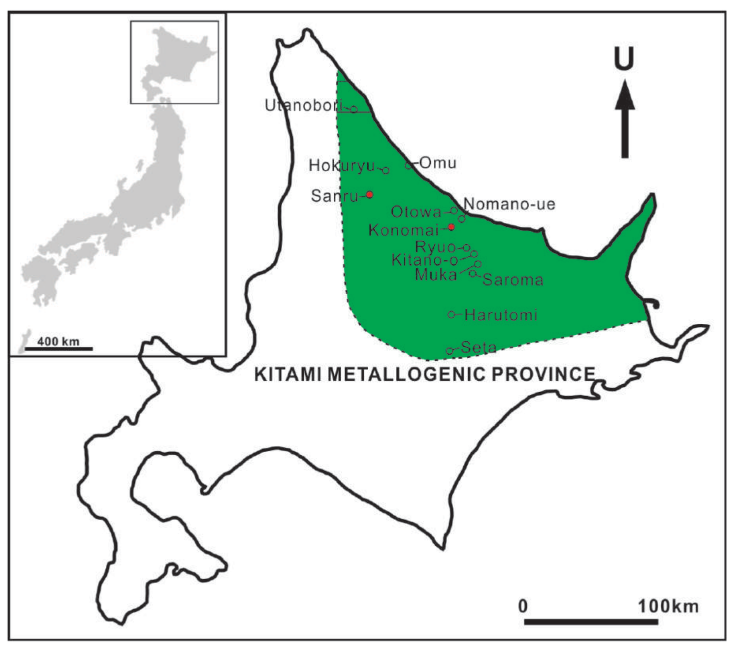

Figure 1. Location map of some epithermal gold-silver vein-type deposits in the Kitami metallogenic province, Hokkaido, Japan (modified after Maeda, 1990).

3. Kitami Metallogenic Province

The Kitami metallogenic province is divided into seven sub-provinces (Urashima, 1961) i.e: the western Kitami, Daisetsu Basement, Spinal Kitami, Kitami-Tokachi, Central Kitami, Abashiri, and Shiretoko mining districts. The province had produced gold, silver, copper, lead, zinc, mercury etc., and especially is known as a gold field (Table 3).

Table 3. Gold and silver production of some economically deposits in the Kitami Province (Ishihara et al., 2000).

Mines	Au (Ton)	Ag (Ton)	Ag/Au
Konomai	73.181	12243	17.0
Hokuryu	2.924	11.268	3.85
Kitano-o	2.916	2.503	0.86
Numano-ue	1.405	94.149	67.0
Sanru	1.340	8.127	6.07
Ikutawara	0.505	3.938	7.80
Tokoro	0.092	2.321	25.2
Muka	0.186	0.814	4.38
Saroma	0.162	0.766	4.73
Ryuo	0.100	0.855	8.55

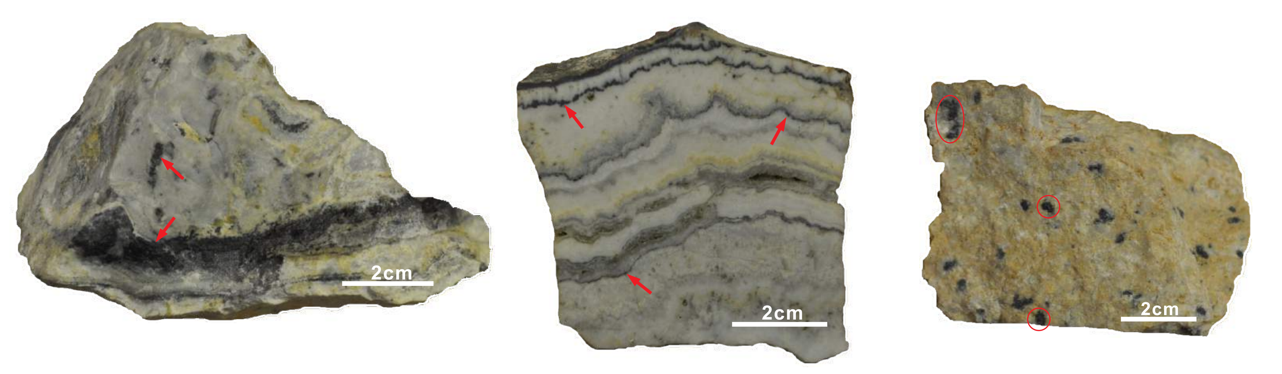

Figure 4. Photographs of some gold-silver ore from Sanru deposit, arrows show the black band containing gold-silver minerals.

2. Regional Geological Setting

Gold, silver, copper and mercury hydrothermal mineralization of the Kitami region at northeastern Hokkaido is related to Middle to Late Miocene back-arc volcanism of the Kuril arc (Watanabe, 1995, Figure 2). The mineralization is mostly in the form of vein but minor disseminated and Kuroko-type deposits were also identified in the Kitami region. Veins-type mineralization strikes mainly in the E-W or NE-SW direction. Strike uniformity in the Kitami region resulted by the existence of constant stress fields prevailing during mineralization (Horikoshi, 1983). Based on paired E-W to ENE-WSW right-lateral and WNW-ESE left-lateral strike-slip shear fractures in the Kitami region, Watanabe (1986) suggested that the region had experienced an E-W trending compressive stress.

The basement rocks of Cretaceous age in this area are the Hidaka group comprising chiefly sandstone and shale, intercalated with conglomerate, acidic tuff, chert, and limestone. The Neogene Tertiary system is composed principally of the middle Miocene Konomai, middle to late Miocene Tomeoka and Shanafuchi (or Shakinzawa) and Quaternary Sawaki Formation in ascending order. Table 1 shows the general geological formations in Central Kitami.

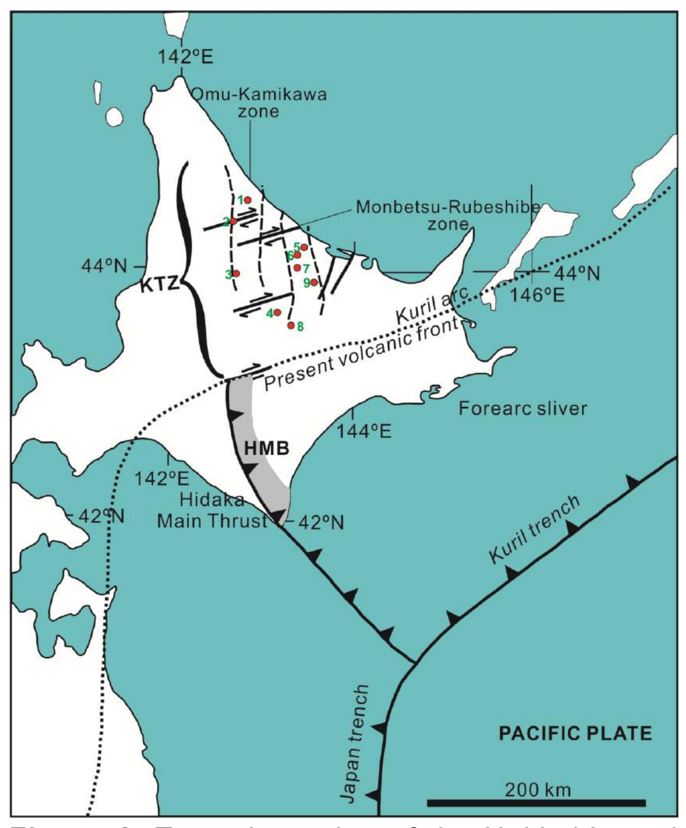

Figure 2. Tectonic setting of the Hokkaido and location of the Kitami region. Names of some major hydrothermal deposits are noted as 1: Hokuryu, 2: Sanru, 3: Tokusei, 4: Itomuka, 5: Numano-ue, 6: Konomai, 7: Kitami, 8: Harutomi, 9: Kitano-o. (Modified after Watanabe, 1996).

Table 1. General geological formations in central Kitami (Urashima, 1957).

Age	Formations
Quarternary	Alluvial and terrace deposits. Sawaki formation - volcanic ash.
Neogene Tertiary	Syanafuchi group { Humi formation - tuff. / Syanafuchi formation - basalt, rhyolite, tuff, and conglomerate. Rhyolite and andesite. Konomai group { Tuff formation. / Tuff and mudstone formation. / Gray shale formation. / Black shale formation.
Mesozoic	Granite. Yubetu group - black shale and sandstone. Hidaka group - black slate, sandstone, schalstein, and diabase.

Table 2. Ages of mineralization and the related rhyolites in some deposits in the Kitami Province.

Name of Ore Deposits	Age of Mineralization	Age of the Related Rhyolite
Sanru	12.4±0.6 Ma*	12.1±0.6 Ma****
Konomai	12.9±0.4 Ma**	12.0±0.6 Ma****
Numano-ue	12.7±0.3 Ma***	12.0±0.6 Ma*****
Ryuo	7.7±0.2 Ma**	
Muka	6.6±0.2 Ma**	
Saroma	5.3±0.5 Ma**	

*Sugaki & Isobe (1985), **Maeda (1990), ***MITI (1994), ****Koshimizu & Kim (1987).

The mineralization ages of epithermal gold-silver vein-type deposits in the Kitami metallogenic province have been studied by Maeda (1990) and Watanabe (1996), based on the K-Ar dating of the vein adularia and quartz mixtures as described in Table 2.

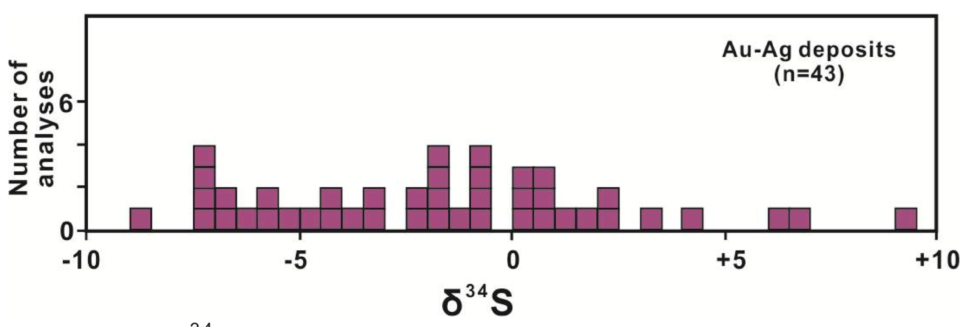

Figure 3. $\delta^{34}S$ values histograms of the sulfide ores of Au-Ag deposits from the northeastern Hokkaido (modified after Ishihara et al., 2000).

Gold-silver deposits of the northeastern Hokkaido have a wide range of $\delta^{34}S$ such as -9.0 to +9.0 per mil (Figure 3). The $\delta^{34}S$ values are especially low (-9.0 ~ 0.7‰) where important ore deposits of Konomai, Hokuryu, Numano-ue and Sanru are distributed. Ishihara et al. (2000) concluded that these low $\delta^{34}S$ values may indicate the existence of reduced-series volcanic rocks in these regions.

4. Ore Mineralogy

Identified gold-silver minerals from the Honpi and Juji-hi veins of Sanru mine with ore microscope and electron probe microanalyzer are aguilarite [Ag_4SeS], naumannite [Ag_2Se], miargyrite [$AgSbS_2$], pyrargyrite [Ag_3SbS_3], stephanite [Ag_5SbS_4], polybasite [$(Ag,Cu)_6(Sb,As)_2S_7$] [Ag_9CuS_4], acanthite [Ag_2S], electrum [Au,Ag], stromeyerite [CuAgS], and silver bearing tetrahedrite associated with clausthalite [PbSe], chalcopyrite[$CuFeS_2$], marcasite [FeS_2], pyrite [FeS_2] and sphalerite [ZnS] (Figure 5). On the other hands, those from Konomai are chalcopyrite, sphalerite, pyrite, marcasite, galena, acanthite, aguilarite, naumannite, pearceite [$(Ag_9CuS_4)(Ag,Cu)_6(As,Sb)_2S_7$], polybasite, pyrargyrite, and stephanite with some secondary minerals of hematite, limonite and covellite (Figure 6).

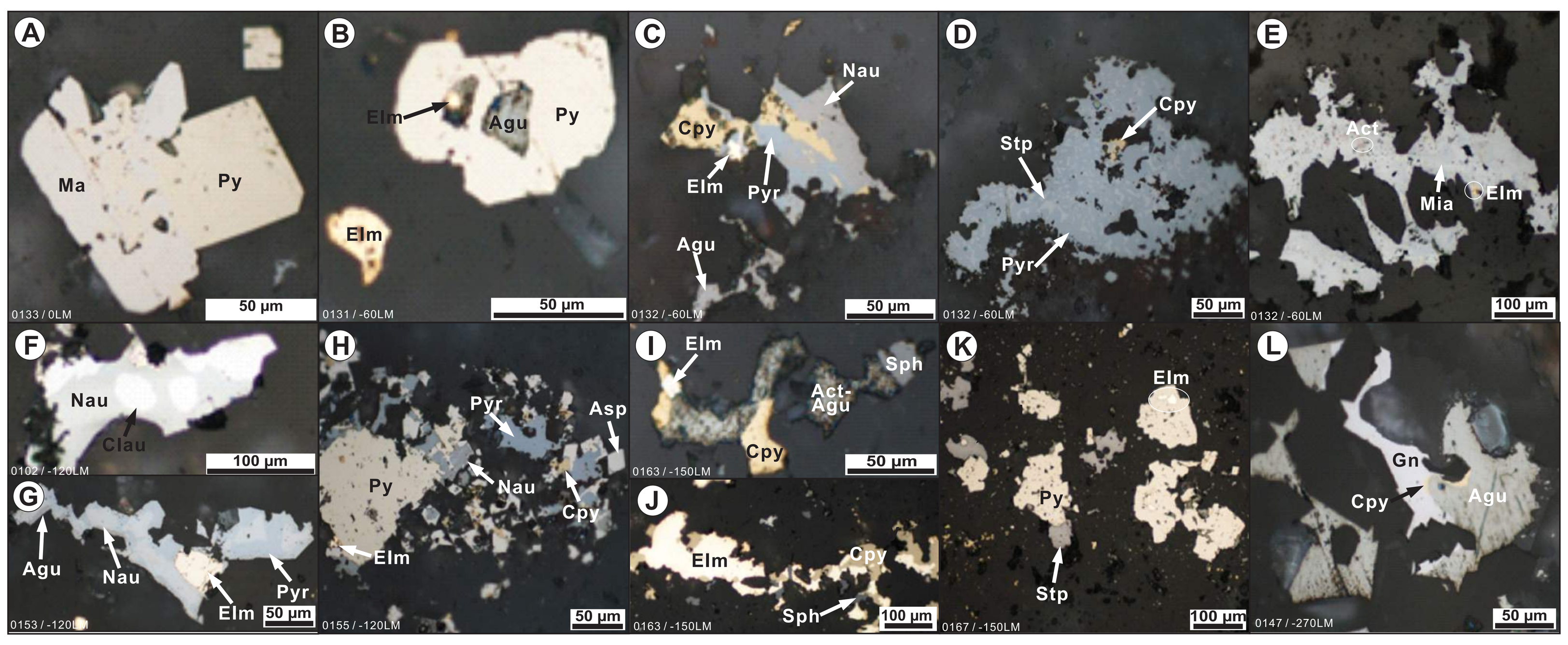

Figure 5. Photomicrographs of gold-silver minerals and their association from the Sanru deposits.
Abbreviations:
Act =acanthite
Agu =aguilarite
Asp =arsenopyrite
Clau =clausthalite
Cpy =chalcopyrite
Elm =electrum
Gn =galena
Ma =marcasite
Mia =miargyrite
Nau =naumannite
Py =pyrite
Pyr =pyrargyrite
Stp =stephanite
Sph =sphalerite

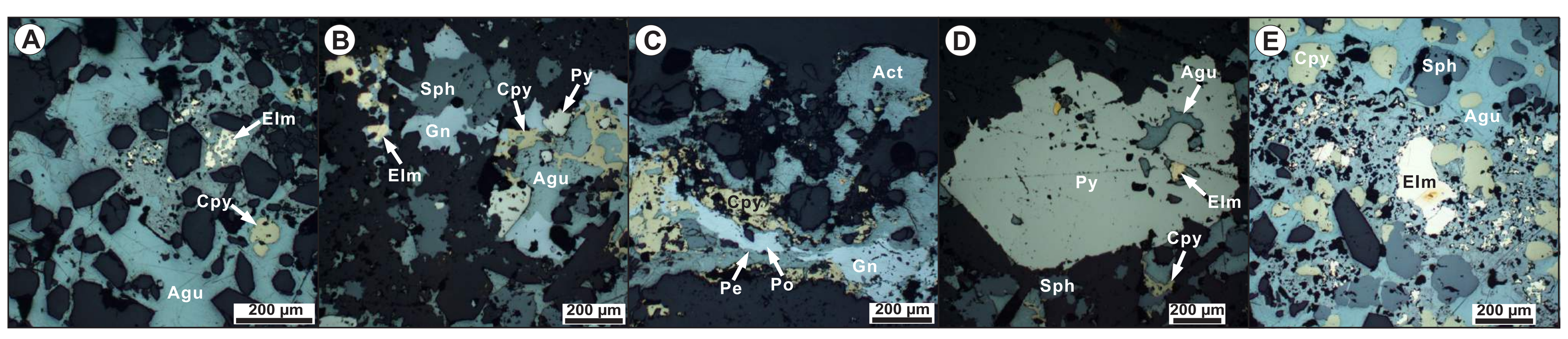

Figure 6. Photomicrographs of gold-silver minerals and their association from the Konomai deposits.
Abbreviations:
Pe = pearceite
Po = polybasite
See figure 5 for other minerals abbreviation name.

Tabel 4. Ore mineral parageneses of samples from Sanru (upper) and Konomai (lower) deposits.

Mineral	Chemical Formula	Paragenetic: Banded Quartz
Naumannite	Ag_2Se	
Aguilarite	Ag_4SeS	
Clausthalite	PbSe	
Arsenopyrite	FeAsS	
Miargyrite	$AgSbS_2$	
Stephanite	Ag_5SbS_4	
Pyrargyrite	Ag_3SbS_3	
Polybasite	$[(AgCu)_6(AsSb)_2S_7][(Ag_9CuS_4)$	
Tetrahedrite	$(Cu,Fe,Ag,Zn)_{12}Sb_4S_{13}$	
Acanthite	Ag_2S	
Chalcopyrite	$CuFeS_2$	
Galena	PbS	
Electrum	Au,Ag	
Pyrite	FeS_2	
Marcasite	FeS_2	
Sphalerite	ZnS	
Stromeyerite	CuAgS	

Mineral	Chemical Formula	Paragenetic: Quartz vein
Naumannite	Ag_2Se	
Aguilarite	Ag_4SeS	
Stephanite	Ag_5SbS_4	
Pyrargyrite	Ag_3SbS_3	
Polybasite	$[(AgCu)_6(AsSb)_2S_7][(Ag_9CuS_4)$	
Pearceite	$(Ag_9CuS_4)(Ag,Cu)_6(As,Sb)_2S_7$	
Acanthite	Ag_2S	
Chalcopyrite	$CuFeS_2$	
Electrum	Au,Ag	
Galena	PbS	
Pyrite	FeS_2	
Sphalerite	ZnS	
Marcasite	FeS_2	

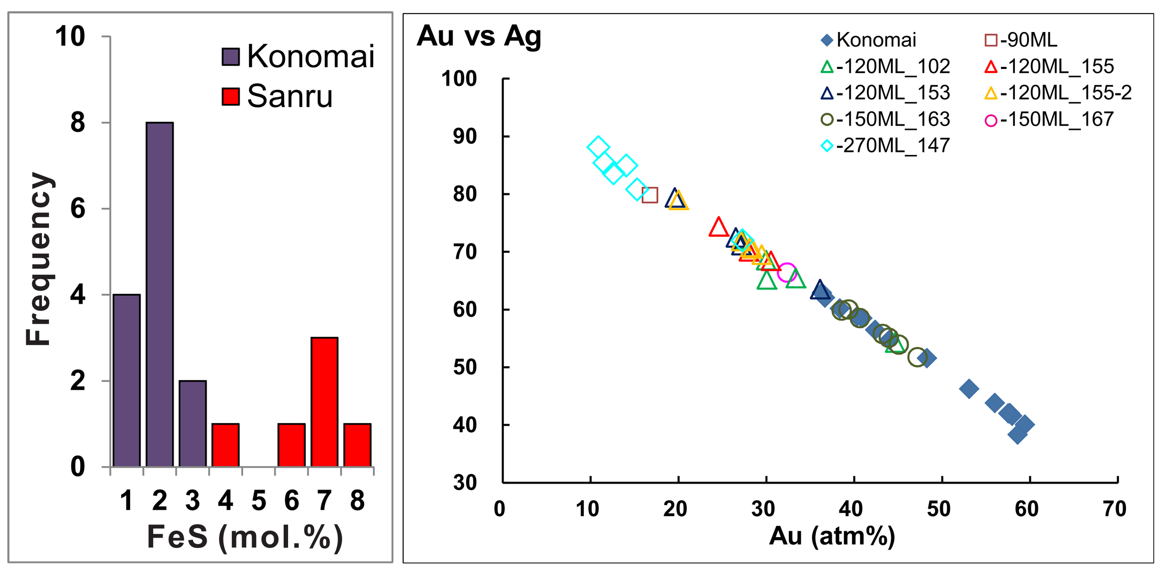

Figure 7. Histogram of Iron contents (mol.% FeS) in sphalerite (left) and graphic of Au-Ag content (atm.%, right) in electrum of ore samples from Sanru and Konomai deposits.

Iron content in sphalerites from both Sanru and Konomai is low (in the ranges of 3.1 - 6.5 and 0.3 - 2.2 mol.% FeS, Figure 7/left). Electrum from Sanru has slightly higher silver content (52 - 88 atm.%) comparing to electrum from Konomai (38 - 63 atm.%, Figure 7/right).

5. Physicochemical Condition of Ore Deposition

Phase relation between temperature, sulfides and selenides proposed by Simon and Essense (1996) is applied to estimate the variations of the physicochemical conditions for the precipitation of selenides and Se-bearing minerals from the Sanru deposit.

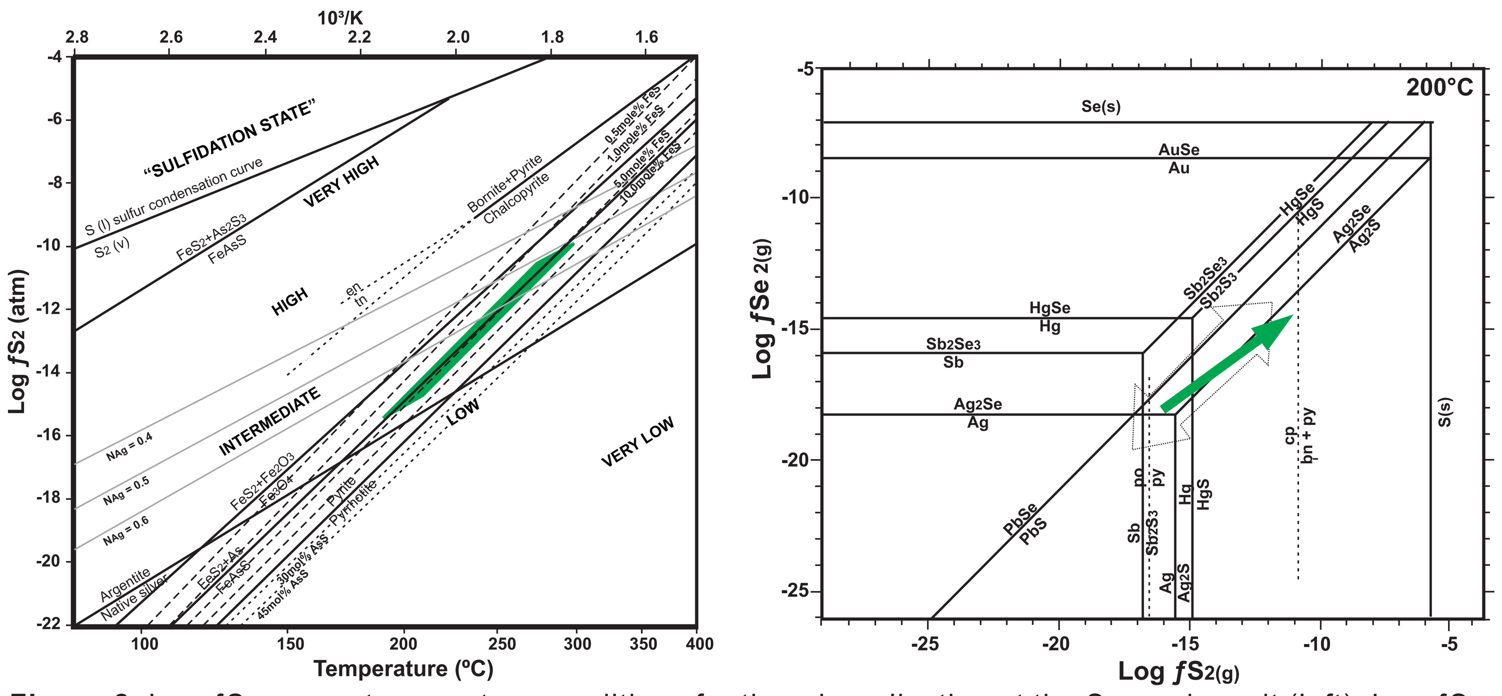

Figure 8. Log fS_2 versus temperature conditions for the mineralization at the Sanru deposit (left). Log fSe_2 versus log fS_2 diagram indicating equilibria between selenides and sulfides of Sanru deposit at 200°C, in vapor saturation.

6. Fluid Inclusion Study

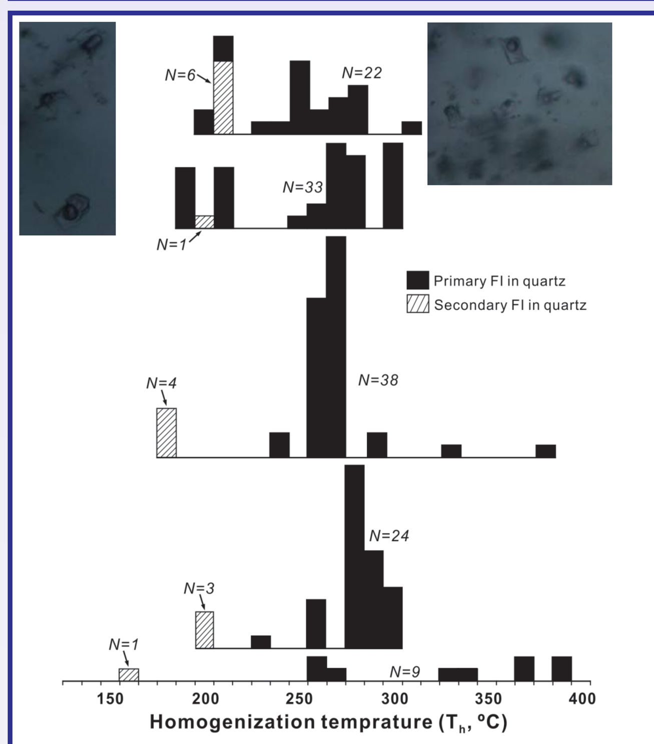

Figure 9. Temperatures formation of Sanru mineralization estimated from fluid inclusions.

Fluid inclusion study of quartz samples from Sanru deposit from -30ML, -60ML, -120ML, -150ML and -270ML concluded the homogenization temperature are in the ranges of 253° - 331°C from the shallower to the deeper part (Figure 9). While, the temperatures required for the formation of the quartz of the Konomai mine based on fluid inclusions study are slightly lower comparing to Sanru, in the ranges of 132°C - 267°C from the early to later stage (Takashima, 1954).

7. Conclusions

The selenides minerals are dominated in the mostly epithermal deposits in the Kitami metallogenic province. The electrum, aguilarite and naumannite are the main Au-Ag minerals in the Sanru and the Konomai mines. No minerals which contain tellurium as main compositions of the minerals have been found at the most of mines in Kitami metallogenic province including in Sanru and Konomai samples, though such minerals often found in the ore deposits of southwestern Hokkaido. Geological setting, intrusions and host rocks might be affected to the ore mineralization in this area.

Acknowledgement

A part of this research is supported by Postdoctoral Fellowship for Foreign Researchers Program funded by JSPS (Japan Society for the Promotion of Science).